GOSPODARKA SUROWCAMI MINERALNYMI

Tom 25 2009 Zeszyt 3

WŁODZIMIERZ FIGIEL*, EWA KAWALEC-LATAŁA**

Context and adaptive transformation applied to interpretation of acoustic pseudoimpedance images of rocky surroundings

Introduction

The hydrocarbon reservoirs are necessary for independence and stability of energy delivery. The most of underground hydrocarbon storage are located in depleted natural gas reservoir. Much more efficient reservoirs are those constructed in rocky salt. Their placement could be in the salt dome, but better localisation due to less complicated geological conditions is in the salt deposits. Rock mass containing salt deposits display high seismologic inhomogeneity. Detection, survey and correct measure of homogeneity of horizontal or semi-horizontal stratum of rocky salt deposits are crucial in preparation of reservoirs. Seismic surface data are the most economical source of information on detected salt deposit inhomogeneity as well as changes of thickness and lithology are subject to visual interpretation. The acoustic pseudoimpedance sections are used to facial lithology changes identification as well as inhomogeneities in geometry, related to thickness changes, dying-out of strata, presence of lenses and so on (Jędrzejowska-Zwinczak 1984).

The acoustic pseudoimpedance is a convolution of real acoustic impedance and seismic wavelet. The pseudoimpedance sections are obtained by the inversion procedure of seismic sections. The basic concept is a reversal of the procedure to compute synthetic seismograms. In practice the inversion procedure is difficult, not unique due to limited frequency bandwidth of seismic data and the presence of noise. Low dominant frequency and especially long signal duration time decrease pseudoimpedance resolution (Kawalec-Latała 2008). In

* Dr inż., Faculty of Mechanical Engineering and Robotics – AGH University of Science and Technology, Cracow.

** Dr inż., Faculty of Geology, Geophysics and Environment Protection, AGH University of Science and Technology, Cracow.

some cases the interpretation is impossible. One of the methods to improve the resolution is thorough processing before the inversion process, especially the deconvolution. The second one is the image processing after the inversion process. In the paper the minimum entropy deconvolution MED before inversion synthetic data generated by INVERS system is applied. MED technique was proposed by Wiggins (Sacchi, Velis Cominquez 1994; Wiggins 1978) and performs maximise an entropy norm so called the Varimax norm.

Image processing tools applied in interpretation of acoustic pseudoimpedance picture are considered as a subject of increase effectiveness of correct interpretation of images simulated by INVERS system (Figiel, Kawalec-Latała 2008).

1. Images simulated by INVERS system for different stratum structure

The real data are briefly distorted especially by transmission losses, random noise, phenomena associated with the recorded seismic signal and band limited wavelet. The main steps in the inversion process are adequate processing seismic data before inversion, visualisation and interpretation. Inhomogeneities of rock mass containing salts deposit have a considerable contrast of elastic properties, so their inner structure can be visible on pseudo – impedance – acoustic – sections. The paper deals with the procedure of improvement of data interpretation in situation low S/N ratio. Pseudoimpedance acoustic sections presented here are generated for low parameter of signal. Additionally on synthetic seismograms the random noise was added.

The algorithm of pseudoimpedance acoustic sections modelling consist of:

- model input data
- calculation of impulse seismogram
- calculation of synthetic seismogram
- calculation of seismogram with noise
- deconvolution MED
- inversion of synthetic seismogram.
- visualization of results by images

Seismological model was created by interpolation of data from two-wells (S-456 and S-475) in Sieroszowice area (Kawalec-Latała, Markiewicz 2008). In the model was assumed hypothetical increase of anhydrite thickness in the bottom of the rock salt. The simplified seismogeological model is presented in Figure 1.

Synthetic seismogram was calculated as a convolution of reflection coefficient series with seismic signal. The signal of Puzyriev $s(t)$ was applied

$$s(t) = \exp(-\beta^2 \cdot t^2) \cdot \sin(2\pi f_0 t \pm \varphi_0) \tag{1}$$

The parameters of signal are: f_0 – dominant frequency, φ_0 – initial phase, β – dumping factor. The ratio f_0/β determine the length of signal. When the ratio is 1 the signal is relatively short; the ratio 2 gives the long signal.

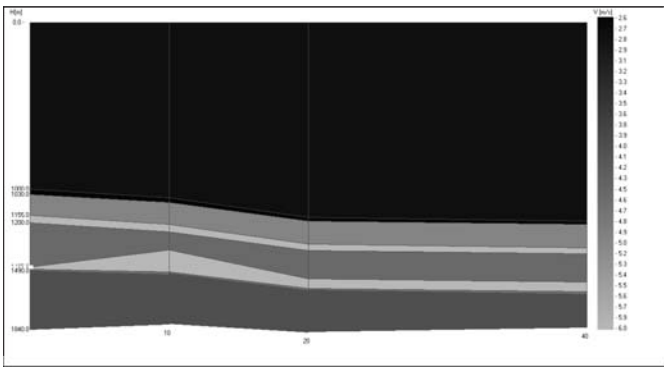

Fig. 1. Simplified seismogeological model based on salt deposit at Sieroszowice area (Nal NW part of LGOM)

Rys. 1. Uproszczony sejsmogeologiczny model wg złoża soli w rejonie Sieroszowic (Nal NW część LGOM)

Synthetic seismic sections were generated for signal with low dominant frequency $f_0 = 40$ Hz and $\beta = 20$ (long signal). The random noise (30%) was added. The data have low S/N ratio. The inversion was done by a recursive method. The section of synthetic acoustic pseudoimpedance is presented in Fig. 2. Synthetic acoustic pseudoimpedance section after the minimum entropy deconvolution (MED) (Broadhead, Pflug; Kawalec-Latała, Markiewicz 2007) done before inversion, is presented in Fig. 3. The colour scale is reflecting the relative velocity (or acoustic impedance) variations. The simplified seismological model for one trace was recalculated for time scale. The reflection coefficients and seismic signal was added to presented synthetic acoustic pseudoimpedance sections. Especially interesting portion of seismic data contains the salts deposits is in time window between 0.8 and 0.94 sec. Figure 2 presents acoustic pseudoimpedance sections without the deconvolution before the inversion.

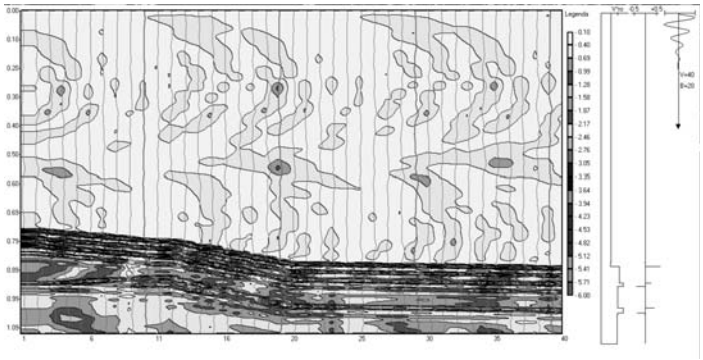

Fig. 2. Synthetic pseudoimpedance acoustic section with simplified seismogeological model for one trace, reflection coefficients and seismic signal. The parameters of signal applied to construction of synthetic seismogram are: – dominant frequency $f_0 = 40$ Hz, – initial phase $\varphi_0 = 0$, – dumping factor $\beta = 20$

Rys. 2. Syntetyczna sekcja pseudoimpedancji akustycznej z wykresem ostatniej trasy uproszczonego modelu sejsmogeologicznego współczynników odbicia i sygnału sejsmicznego

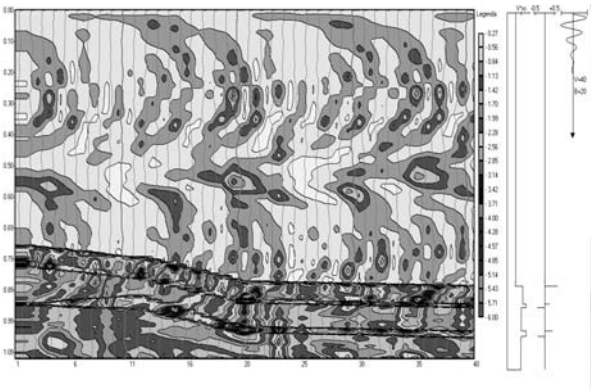

Fig. 3. Synthetic pseudoimpedance acoustic section after MED deconvolution with simplified seismological model for one trace, reflection coefficients and seismic signal vs. time

Rys. 3. Syntetyczna sekcja pseudoimpedancji akustycznej po dekonwolucji MED z wykresem ostatniej trasy uproszczonego modelu sejsmogeologicznego współczynników odbicia i sygnału sejsmicznego w czasie

The analysis of above presented synthetic pseudoimpedance acoustic section shows how the minimum entropy deconvolution MED done before inversion process influences of the image quality. It is necessary to underline, that image is constructed for: low S/N data rate (model simulate high noise and low signal parameters), low dominant frequency and long seismic signal (the ratio $f_0 / \beta \geq 2$). In many cases deconvolution improve the resolution but the effect can be sometimes insufficient. In such cases the image processing tools applied to process pseudoimpedance acoustic picture may increase effectiveness of correct interpretation.

2. Convolution and context filter applied to images generatedby INVERS system

Image restoration is difficult since it is an ill-posed inverse problem: there is not enough information in the degraded image to determine the original image unambiguously. The most frequently used geometric conversions of image with computer aid technique there are: point transformation, context and spectrum transformation as well different form of a morphology mapping (Boyle, Sonka, Hlavac 1993; Broadhead, Pflug).

Context transformation bases on alteration of image elements depending on their own content and content of circumambient elements. Context transformation required many calculation and recalculation on bases of surrounding image elements to achieve value of transformed image element. Those operations are defined by convolution function. Convolution provides a way of `multiplying together' two arrays of numbers, generally of different sizes, but of the same dimensionality, to produce a third array the same dimensionality. This can be used in image processing to implement operators whose output pixel values are simple linear combinations of certain input pixel values.

In an image context processing, one of the input arrays is normally just a greyscale. The second array is usually much smaller, and is also two-dimensional, and is known as the kernel.

I_{11}	I_{12}	I_{13}	I_{14}	I_{15}	I_{16}	I_{17}	I_{18}	I_{19}
I_{21}	I_{22}	I_{23}	I_{24}	I_{25}	I_{26}	I_{27}	I_{28}	I_{29}
I_{31}	I_{32}	I_{33}	I_{34}	I_{35}	I_{36}	I_{37}	I_{38}	I_{39}
I_{41}	I_{42}	I_{43}	I_{44}	I_{45}	I_{46}	I_{47}	I_{48}	I_{49}
I_{51}	I_{52}	I_{53}	I_{54}	I_{55}	I_{56}	I_{57}	I_{58}	I_{59}
I_{61}	I_{62}	I_{63}	I_{64}	I_{65}	I_{66}	I_{67}	I_{68}	I_{69}

k_{11}	k_{12}	k_{13}
k_{21}	k_{22}	k_{23}
k_{31}	k_{32}	k_{33}

Fig. 4. An example small image (left) and kernel (right) to illustrate convolution. The labels within each grid square are used to identify each square

Rys. 4. Przykład małego obrazu (po lewej) i jądra (po prawej) dla ilustracji konwolucji. Etykiety w każdym kwadracie siatki są używane do identyfikacji kwadratu

The convolution is performed by sliding the kernel over the image, generally starting at the top left corner, so as to move the kernel through all the positions where the kernel fits entirely within the boundaries of the image (Boyle, Sonka, Hlavac 1993; Figiel, Kawalec--Latała 2008). Each kernel position corresponds to a single output pixel, the value of which is calculated by multiplying together the kernel value and the underlying image pixel value for each of the cells in the kernel, and then adding all these numbers together.

Mathematically we can write the convolution as:

$$O(i,j) = \sum_{k=1}^{m} \sum_{l=1}^{n} I(i+k-1, j+L-1)K(k,l) \tag{2}$$

where:

i runs from 1 to $M - m + 1$ and j runs from 1 to $N - n + 1$.

Convolution can be used to implement many different operators, particularly spatial filters and feature detectors and in our case median filter.

An example pictures of INVERS system model A42s30 – with ill-posed parameters as: low main frequency $f = 40$ [Hz], dumping factor $\beta = 20$, noise s = 30% are presented in tree phases i.e. as portray chart of original matrix and after cutting off percentils (1.99), mash visualisation and contour image after median filtering.

The median and mean filtering methods will reduce the amount of noise contained in a signal, but will do nothing towards restoring a distorted image. It is a low-pass filtering method based on the assumption that each pixel is more or less like the ones around it. As a result, fine details may be loss, but a better feel for the entire image may be gained (Pitas, Ioannis 1993)). The results achieved on that stage of image processing are far away of

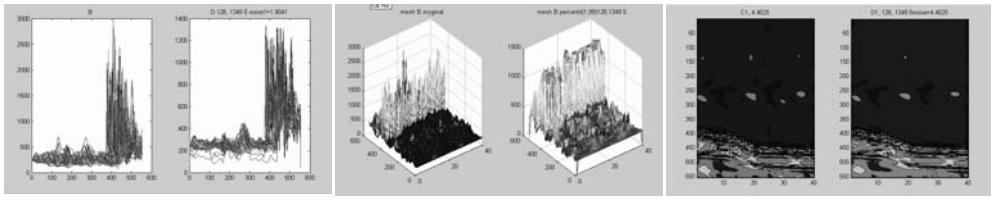

a) b) c)

Fig. 5. The sample of median filtering process of image model A42S30
a) as portray chart of original matrix and after cutting off percentils (1.99), b) mash visualisation c) contour image after median filtering

Rys. 5. Przykład efektów procesu filtrowania obrazu modelu A42S30
a) wykres portretowy oryginalnej macierzy i po odcięciu percentyli (1,99), b) wizualizacja siatki przestrzennej, c) wykres konturowy po filtracji medianowej

pictures easy to interpretation. Considered in our paper images, are degraded by additive noise and blurring so we introduce concept of using Wiener filter. That filter is the MSE (mean square error) – optimal stationary linear filter.

Calculation of the Wiener filter requires the assumption that the signal and noise processes are second-order stationary (Gaskill 1978). In the paper, we consider only noise processes with zero mean value.

Wiener filters are usually applied in the frequency domain. Given a degraded image $x(n,m)$, we takes the Discrete Fourier Transform (DFT) to obtain $X(u,v)$. The original image spectrum is estimated by taking the product of $X(u,v)$ with the Wiener filter $G(u,v)$:

$$\hat{S}(u,v) = G(u,v)X(u,v) \tag{3}$$

The inverse DFT is then used to obtain the image estimate from its spectrum. The Wiener filter is defined in terms of these spectra:

$H(u,v)$ – Fourier transform of the point-spread function (PSF),

$P_s(u,v)$ – power spectrum of the signal process, obtained by taking the Fourier transform of the signal autocorrelation,

$P_n(u,v)$ – power spectrum of the noise process, obtained by taking the Fourier transform of the noise autocorrelation.

The Wiener filter is:

$$G(u,v) = \frac{H^*(u,v)P_s(u,v)}{|H(u,v)|^2 P_s(u,v) + P_n(u,v)} \tag{4}$$

Dividing thorough by P_s makes its behaviour easier to explain:

$$G(u,v) = \frac{H^*(u,v)}{|H(u,v)|^2 + \frac{P_n(u,v)}{P_s(u,v)}} \tag{5}$$

The term P_n/P_s can be interpreted as the reciprocal of the signal-to-noise ratio. Where the signal is very strong relative to the noise, $P_n/P_s \cong 0$ and the Wiener filter becomes $H^{-1}(u,v)$ – the inverse filter for the PSF. Where the signal is very weak, $P_n/P_s \Rightarrow \infty$ and $G(u,v) \Rightarrow 0$

For the case of additive white noise and no blurring, the Wiener filter simplifies to:

$$G(u,v) = \frac{P_s(u,v)}{P_s(u,v) + \sigma_n^2} \quad \text{where } \sigma_n{}^2 \text{ is the noise variance} \tag{6}$$

Wiener filters are unable to reconstruct frequency components that have been degraded by noise (Gonzales, Wintz 1987). They can only suppress them. To speed up filtering, can be taken the inverse FFT of the Wiener filter $G(u,v)$.

Application of Wiener filter with inverse FFT in MTLAB code permit us gather results of transformed images for earlier model origin matrix of acoustic pseudoimpedance. Evaluation of achieved results are made by comparison of images before transformation and after two phase processing i.e. median filtering as first phase and Winer filtering as second phase.

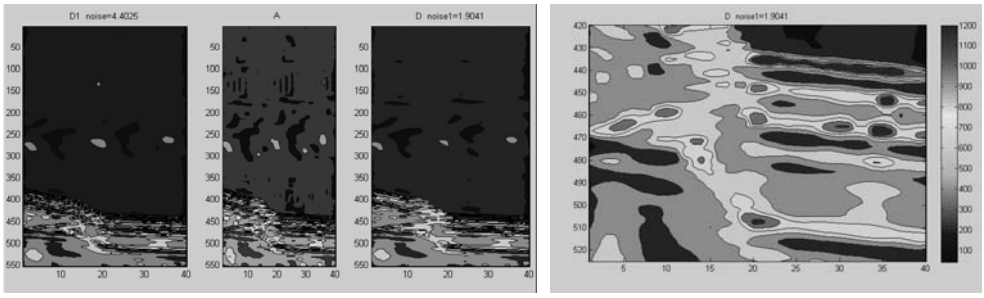

Fig. 6. Model A42S3 as origin matrix picture, after median filter operation and finally as Winer filtering result. Part on right side depicts magnification of the most interesting part (anhydrite seam-like stratum) of original image of geomorphologic section

Rys. 6. Model A42S30 jako obraz oryginalnej macierzy, po filtracji medianowej i na końcu jako rezultat filtracji Wienera. Po prawej stronie, powiększenie najbardziej interesujacej części (pozioma warstwa anhydrytu) oryginalnego obrazu geomorfologicznego przekroju

Because, presented results are still out of our expectation, considering ability to facial lithology identification of anhydrite in simulated picture of acoustic pseudoimpedance matrix, our idea are turned to edge identification in image processing.

3. Algorithms of edge detection used to filtering difficult cases of noisy INVERS images

Edge detection in image processing is based on few algorithms described, between other, by Sobel and Prewitt operator as well as defined by Laplacian of Gaussian method (Hunt 1973).

The **Sobel** operator technically is a discrete differentiation operator, computing an approximation of the gradient of the image intensity function. At each point in the image, the result of the Sobel operator is either the corresponding gradient vector or the norm of this vector. The Sobel operator is based on convolving the image with a small, separable, and integer valued filter in horizontal and vertical direction. The Sobel operator is relatively crude (in particular for high frequency variations) in the image.

Mathematically, the operator uses two 3×3 kernels which are convolved with the original image to calculate approximations of the derivatives – one for horizontal changes, and one for vertical. If we define A as the source image, and G_x and G_y are two images which at each point contain the horizontal and vertical derivative approximations, the computations are as follows:

$$G_y = \begin{bmatrix} +1 & +2 & +1 \\ 0 & 0 & 0 \\ -1 & -2 & -1 \end{bmatrix} * A \qquad G_x = \begin{bmatrix} +1 & 0 & -1 \\ +2 & 0 & -2 \\ +1 & 0 & -1 \end{bmatrix} * A \tag{7}$$

where

* here denotes the 2-dimensional convolution operation.

The x-coordinate is here defined as increasing in the "right"-direction, and the y-coordinate is defined as increasing in the "down"-direction. At each point in the image, the resulting gradient approximations can be combined to give the gradient magnitude, using G calculation and calculate θ the gradient's direction

$$G = \sqrt{G_x^2 + G_y^2}; \qquad \theta = \arctan\left(\frac{G_y}{G_x}\right) \tag{8}$$

where, for example, Θ is 0 for a vertical edge that is darker on the left side.

The Sobel operator represents a rather inaccurate approximation of the image gradient, but is still of sufficient quality to be of practical use in many applications. It uses intensity values only in a 3×3 region around each image point to approximate the corresponding image gradient, and it uses only integer values for the coefficients which weight the image intensities to produce the gradient approximation.

Prewitt is a method of edge detection in image processing that calculates the maximum response of a set of convolution kernels to find the local edge orientation for each pixel. Various kernels can be used for this operation. Taking one of the kernels and rotating its coefficients circularly produces the whole set of 8 kernels. Each of the resulting kernels is sensitive to an edge orientation ranging from 0° to 315° in steps of 45°, where 0° corresponds to a vertical edge. The maximum response for each pixel is the value of the corresponding

pixel in the output magnitude image. The values for the output orientation image lie between 1 and 8, depending on which of the 8 kernels produced the maximum response.

The Prewitt edge detector is an appropriate way to estimate the magnitude and orientation of an edge. Mathematically, the operator uses two 3×3 kernels which are convolved with the original image to calculate approximations of the derivatives – one for horizontal changes, and one for vertical. If we define A as the source image, and G_x and G_y are two images which at each point contain the horizontal and vertical derivative approximations, the latter are computed as:

$$G_y = \begin{bmatrix} -1 & 0 & +1 \\ -1 & 0 & +1 \\ -1 & 0 & +1 \end{bmatrix} * A \qquad G_x = \begin{bmatrix} -1 & -1 & -1 \\ 0 & 0 & 0 \\ +1 & +1 & +1 \end{bmatrix} * A \tag{9}$$

The Laplacian is a 2-D isotropic measure of the 2nd spatial derivative of an image. The Laplacian of an image highlights regions of rapid intensity change and is therefore often used for edge detection (Boyle, Sonka, Hlavac 1993; Pitas 1993). The Laplacian is often applied to an image that has first been smoothed with something approximating a Gaussian smoothing filter in order to reduce its sensitivity to noise, and hence the two variants will be described together here. The operator normally takes a single graylevel image as input and produces another graylevel image as output.

The Laplacian $L(x,y)$ of an image with pixel intensity values $I(x,y)$ is given by:

$$L(x, y) = \frac{\partial^2 I}{\partial x^2} + \frac{\partial^2 I}{\partial y^2} \tag{10}$$

This can be calculated using a convolution filter.

Since the input image is represented as a set of discrete pixels, we have to find a discrete convolution kernel that can approximate the second derivatives in the definition of the Laplacian. Two commonly used small kernels are shown in Figure 7.

0	–1	0
–1	4	–1
0	–1	0

–1	–1	–1
–1	8	–1
–1	–1	–1

Fig. 7. Two matrix commonly used discrete approximations to the Laplacian filter

Rys. 7. Dwie, powszechnie używane macierze dla dyskretnych aproksymacji w filtrach Laplasa

Using one of these kernels, the Laplacian can be calculated using standard convolution methods. These kernels are very sensitive to noise. To counter this, the image is often Gaussian smoothed before applying the Laplacian filter. Since the convolution operation is

associative, we can convolve the Gaussian smoothing filter with the Laplacian filter first of all, and then convolve this hybrid filter with the image to achieve the required result.

Doing things this way has two advantages:

— Since both the Gaussian and the Laplacian kernels are usually much smaller than the image, this method usually requires far fewer arithmetic operations.

— The LoG (`Laplacian of Gaussian') kernel can be precalculated in advance so only one convolution needs to be performed at run-time on the image.

The 2-D LoG function centered on zero and with Gaussian standard deviation σ has the form:

$$LoG(x, y) = -\frac{1}{\pi\sigma^4}\left[1-\frac{x^2+y^2}{2\sigma^2}\right]e^{\frac{x^2+y^2}{2\sigma^2}} \tag{11}$$

and is shown in Figure 8.

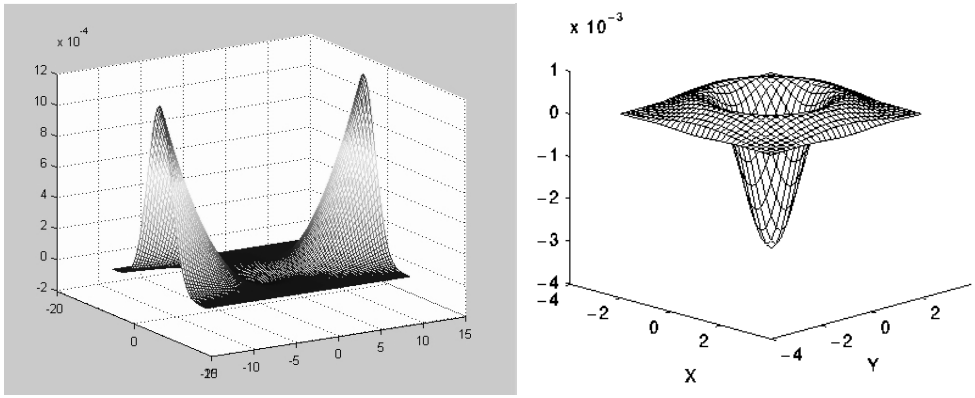

a) **b)**

Fig. 8. The 2-D Laplacian of Gaussian (LoG) function
a) The *x* and *y* axes are marked in standard deviations σ, b) Fragment the 2-D LoG in centre part

Rys. 8. Funkcja Laplasianu Gaussa (LoG) dwuwymiarowa
a) Wartości osi *x* i *y* są wyskalowane w krotnościach odchylenia standardowego σ, b) Fragment funkcji 2-D LoG w centralnej części

A discrete kernel that approximates this function (for a Gaussian σ = 1.4) is shown in Figure 9.

As the Gaussian is made increasingly narrow, the LoG kernel becomes the same as the simple Laplacian kernels shown in Fig. 8b. This means that at a reasonably sharp edge between two regions of uniform but different intensities, the LoG response will be:

— zero at a long distance from the edge,

— positive just to one side of the edge,

0	1	1	2	2	2	1	1	0
1	2	4	5	5	5	4	2	1
1	4	5	3	0	3	5	4	1
2	5	3	-12	-24	-12	3	5	2
2	5	0	-24	-40	-24	0	5	2
2	5	3	-12	-24	-12	3	5	2
1	4	5	3	0	3	5	4	1
1	2	4	5	5	5	4	2	1
0	1	1	2	2	2	1	1	0

Fig. 9. Discrete approximation matrix to LoG function with Gaussian $\sigma = 1.4$

Rys. 9. Macierz dyskretnej aproksymacji dla funkcji LoG z funkcją Gaussa $\sigma = 1.4$

— negative just to the other side of the edge,
— zero at some point in between, on the edge itself.
Figure below illustrates the response of the LoG to a step edge.

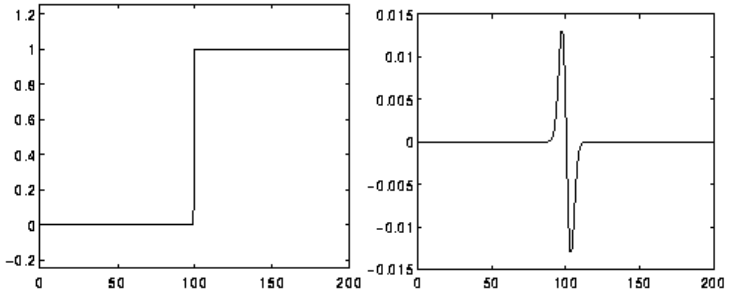

Fig. 10. Response of 1-D LoG filter to a step edge. The left-hand graph shows a 1-D image, 200 pixels long, containing a step edge. The right hand graph shows the response of a 1-D LoG filter with Gaussian $\sigma = 3$ pixels

Rys. 10. Jednowymiarowa odpowiedź filtracji LoG na skok jednostkowy. Wykres z lewej strony pokazuje jednowymiarowy obraz, 200 pikseli zawierające skok jednostkowy. Wykres z prawej strony pokazuje efekt filtracji LoG z funkcją Gaussa $\sigma = 3$ piksele

By itself, the effect of the filter is to highlight edges in an image.

The sample results, obtained from our calculation (on model A42S30 considered in the paper), are gathered on picture below. The original matrix of acoustic pseudoimpedance up to now be pictured as colourful image. MATLAB function used to use a greyscale image, so original matrix was recalculated to limited range of value (0-255) corresponding to greyscale. After that normalisation process, acoustic pseudoimpedance matrix was filtered by edge detecting algorithms, described before. The sample results are presented on picture below.

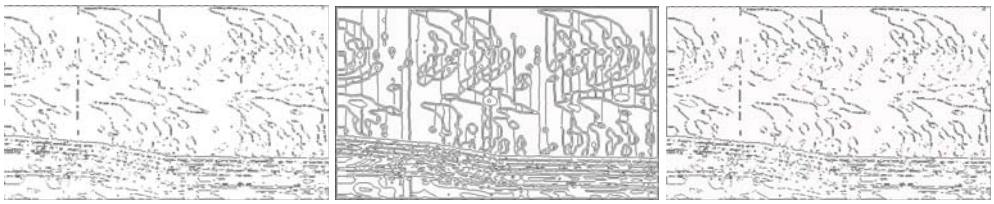

Fig. 11. Original acoustic pseudoimpedance matrix of model A42S30 after process edge detection with a) Prewitt, b) Canny and c) Sobel algorithms accordingly

Rys. 11. Oryginalna macierz pseudoimpedancji akustycznej dla modelu A42S30 po procesie wykrywania krawędzi metodą
a) Prewitta, b) Canny i c) Sobela

Reading ability of the above images and proper their geological interpretation is doubtful still so next step of investigation is idea to detect edges of images after process filtering described in chapter 3 of our paper.

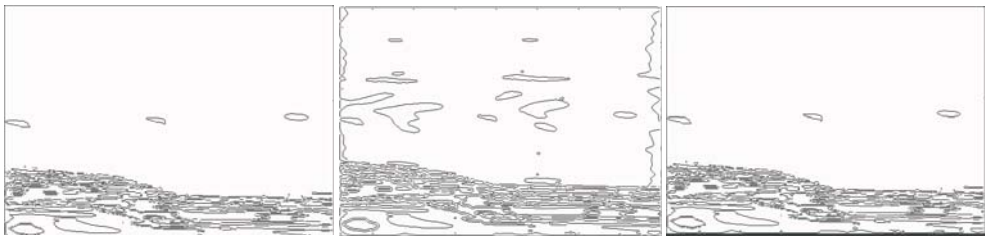

Fig. 12. The acoustic pseudoimpedance matrix image of model A42S30 after median/Wiener filtering process transformed by edge detection with Prewitt, Canny and Sobel algorithms accordingly

Rys. 12. Macierz pseudoimpedancji akustycznej modelu A42S30 po procesie filtracji medianowej /Wienera i procesie wykrywania krawędzi według algorytmu: Prewitta, Canny i Sobela

Reading ability of those images and proper their geological interpretation is little more accurate comparing to previous results, but sill not enough to fill satisfaction. It should be kept in memory, that original image and their matrix belongs to difficult objects. Its parameters not allow to easy interpretation, and detection of interesting stratum for example layer of rocky salt or anhydrite is still doubtful. Our investigation concept was direct to consider process of sliding mash charts of acoustic pseudoimpedance matrix value on chosen level, proper for interesting stratum. The results are present as contour charts fillet with colour depending on acoustic pseudo impedance value. The sample results for anhydrite stratum in considered model A42S30 generated from INVERS system is depicted below.

As can be observed on Fig. 14, anhydrite layers are market as colour contours of few layers (according with colour scale on right side) for relative value of acoustic velocity from 760 to 840. Those pictures may be decompose and presented as colour filled separated pictures – handy for reading and interpretations.

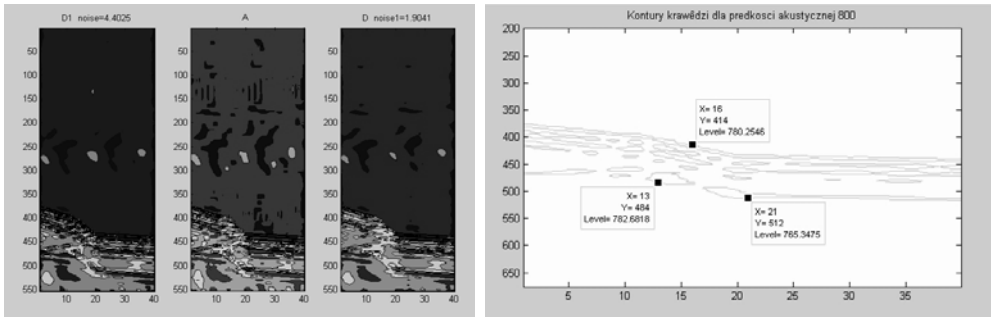

Fig. 13. The sample results for anhydrite stratum in considered model A42S30 generated from INVERS system

Rys. 13. Przykładowe wyniki dla warstwy anhydrytu w rozważanym modelu A42S30 wygenerowanym w systemie INVERS

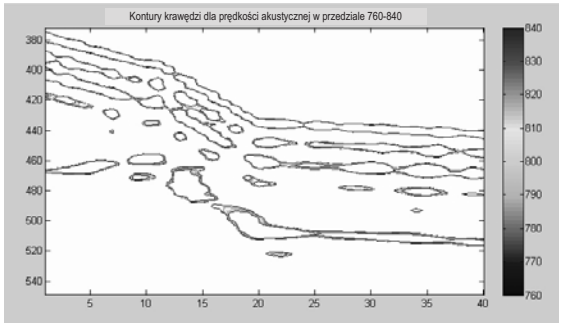

Fig. 14. The magnitude of same sample of anhydrite stratum in considered model A42S30 generated from INVERS system

Rys. 14. Powiększony obraz przykładowych wyników dla warstwy anhydrytu w rozważanym modelu A42S30 wygenerowanym przez INVERS system

4. Resume of results and conclusions

The energetic independence is strategic goal of current policy of all state administrations. That facts imply development of indefecttible hydrocarbon reservoirs, frequently exploited in depleted gas reservoirs or constructed in seam-like salt deposits. Detection and identification of salt stratum homogenity (required as reservoir construction parameters) may be executed by seismic surface measurement and calculations of seismic section inversion leading to approximation of distribution of acoustic impedance. The results are validated as image quality, which for some signal and noise conditions are improved by use of minimum entropy deconvolution method. The investigation results, presented in the paper, proof serviceability of MED method to resolution increase and correct interpretation of geologic section images. Unfortunately in some cases, the inversion procedure is difficult, not unique due to limited frequency bandwidth of seismic data and the presence of noise. Even minimum

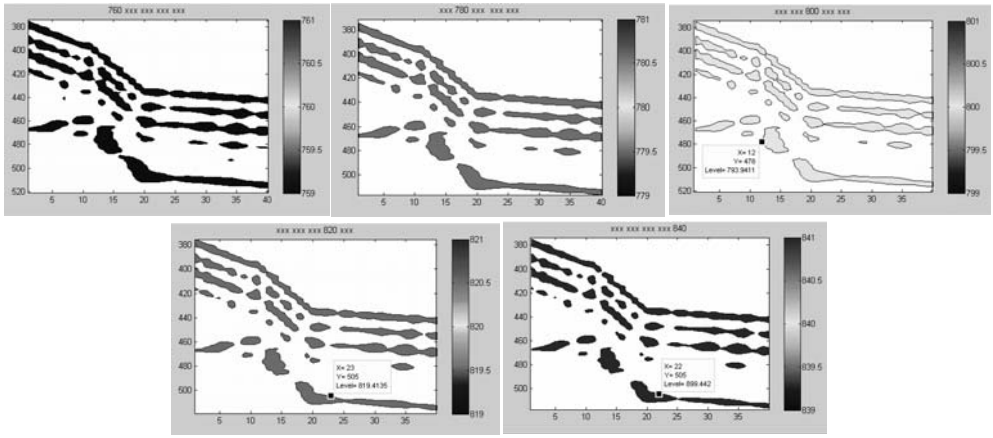

Fig. 15. Picture of anhydrite stratum (selected set of impedance) from considered model A42S30 received by decomposition of original image matrix generated by INVERS system

Rys. 15. Obraz warstwy anhydrytu (wybrany zestaw wartości impedancji) w rozważanym modelu A42S30 otrzymany przez dekompozycję oryginalnej macierzy generowanej przez system INVERS

entropy deconvolution method image improvements not assure satisfying correctness of interpretation for full range conditions.

Analysis and results presented in above paper are prepared on model as standard salt deposit in our country. The models of synthetic section, generated for considered geological configuration of salt deposit with anhydrite and secondary salt deposit intercalation were study materials for parameter selection of image processing. Into presented outcome, were chosen boundary bed conditions of seismology measurement signal i.e. low main frequency $f = 40$ Hz, little dump coefficient $\beta = 20$, and relatively high noise level $\eta = 30\%$. That difficult conditions were assumed as real measurement signal condition and determine degree of method applicability in proper interpretation of considered pseudoimpedance acoustic section of seismic-geology images. Conclusions of conducted investigation suggest prudence, because contexts filtering even complying adaptive filters are sensitive on context extent. In present stage of investigation, a choice of context extent was select by evaluation of analysed image interpretation easiness. Applications of Wiener algorithm enrich process analysis and conduct to better results. The best results of Wiener filtering can be obtain for determined noise parameters, what is in real measurement difficult. Presented results required improvement considering ability to facial lithology identification of anhydrite in simulated images of acoustic pseudoimpedance matrix. One of ideas considered in paper is method of edge identification in image processing.

In presented our paper, we detect edges of analysed images using Sobel operator, Prewitt operator as well as Laplacian of Gaussian method and by slicing 3-D acoustic pseudoimpedance matrix on proper acoustic pseudoimpedance value, corresponding to selected geologic stratum.

The Sobel operator is based on convoluting the image with a small, separable, and integer valued filter in horizontal and vertical direction so the gradient approximation which it

produce is relatively crude. Its advantage is its relatively inexpensiveness in terms of computations.

The Prewitt method is called edge template matching, because a set of edge templates is matched to the image, each representing an edge in a certain orientation. The edge magnitude and orientation of a pixel is determined by one form eight template that matches the local area of the pixel the best.

The result for the edge magnitude image is very similar with both (Sobel and Prewitt) methods, provided the same convoluting kernel is used.

The Laplacian, as isotropic measure on plane of the 2nd spatial derivative of an image, highlights regions of rapid intensity change and therefore is used in our analysis for edge detection. The Laplacian is applied to investigate image that has first been smoothed with Wiener smoothing filter in order to reduce its sensitivity to noise.

The sliding process of mash chart of acoustic pseudoimpedance matrix value on chosen level, proper for interesting stratum has got most interesting results. The images of selected stratum (anhydrite) are presented as contour charts fillet with colour depending on value of acoustic pseudoimpedance (set of few value for given range).

REFERENCES

Boyle R., Sonka M., Hlavac V., 1993 – Image Processing, Analysis, and Machine Vision. First Edition, University Press, Cambridge.

Broadhead M.K., Pflug L.A. – Deconvolution for transient classification using fourth order statistics. Naval Research Laboratory, Acoustics Division, Stennis Space Center, MS 39529-5009, USA.

Figiel W., Kawalec-Latała E., 2008 –Analiza obrazów sekcji pseudo impedancji akustycznej. Górnictwo i Geoinżynieria t. 32, z. 1, s. 65–72.

Figiel W., Kawalec-Latała E., 2008 – Zastosowanie analizy i przetwarzania obrazów do interpretacji syntetycznych sekcji pseudoimpedancji akustycznej. Gospodarka Surowcami Mineralnymi t. 24, z. 2/3, s. 371–385.

Gaskill J.D., 1978 – Linear Systems, Fourier Transforms, and Optics, John Wiley and Sons, Inc., New York.

Gonzales R.C., Wintz P., 1987 – Digital Image Processing, Second Edition, Addison-Wesley Publishing Co., Massachusets.

Hunt B.R., 1973 – The Application of Constrained Least Squares Estimation to Image Restoration by Digital Computer, IEEE Transactions on Computers, Vol C-22, No. 9, September 1973.

Jędrzejowska-Zwinczak H., 1984 – Zastosowanie metody sejsmoakustycznej w zagadnieniach prognozowania przekroju geologicznego. Prace IGNiG nr 52, s. 105–123.

Kawalec-Latała E., Markiewicz A., 2007 – Zastosowanie syntetycznych sekcji pseudo impedancji akustycznej do odwzorowania geologii w rejonie potencjalnej budowy tawernowego magazynu węglowodorów w soli Nal NW części LGOM. Geotechnika w budownictwie i górnictwie (prace naukowe Inst. Geotechniki. i Hydrotechniki Politechniki Wrocławskiej), nr 76, s. konf. 42, s. 315–323.

Kawalec-Latała E., 2008 – The influence of seismic wavelet on the resolution of pseudo impedance section for construction of underground storage. Gospodarka Surowcami Mineralnymi t. 24, z. 2/3, s. 387–397.

Pitas J.I., 1993 – Digital Image Processing Algorithms, Prentice Hall International (UK) Ltd., Cambridge.

Sacchi M.D., Velis D.R., Cominguez A.H., 1994 – Minimum entropy deconvolution with frequency--domain constraints, Geophysics vol.59, no 6, p.938-945, June 1994.

Wiggins R.A., 1978 – Minimum Entropy Deconvolution. Geoexploration vol. 16, pp. 21–35.

CONTEXT AND ADAPTIVE TRANSFORMATION APPLIED TO INTERPRETATION OF ACOUSTIC PSEUDOIMPEDANCE IMAGES OF ROCKY SURROUNDINGS

Key words

Hydrocarbon storage, seismic surface measurement, distribution of acoustic pseudoimpedanc, data analysis and visualisation, context and adaptive transformation of images, rock section structure interpretation inhomogeneity detection

Abstract

Underground hydrocarbon storage plays an important role in the world. The most of them is located in depleted natural gas reservoirs. Rocky salt deposits with homogenous inner structure and horizontal or semi-horizontal stratum may be the best for future plans of under ground reservoir localisation. Within salt deposit, stratum inhomogeneity as well as changes of thickness and lithology should be especially examined and predicted before the underground reservoir location plan is fixed. Seismic surface measurement data are the most economical source of such information. Calculations of seismic section inversion leads to approximation of distribution of acoustic pseuoimpedance. The pseudoimpedance acoustic sections analysis and visualisation are effective ways to stratum homogeneity identification goal. In this paper, the improvement of geologic section image resolution by use of minimum entropy deconvolution method before inversion (for synthetic data generated by INVERS system) is applied. The authors propose context and adaptive transformation of images also as a way to increase the effectiveness of correct interpretation of simulated images. The paper introduces the algorithms of visual trans- formation and analysis of results to define quality of rock section structure interpretation. The goal of the study is to develop applications of image transformation tools to inhomogeneity detection of lithology-phacial structure of seam-like salt deposits.

TRANSFORMACJA KONTEKSTOWA I ADAPTACYJNA STOSOWANA W INTERPRETACJI OBRAZÓW PSEUDOIMPEDANCJI AKUSTYCZNEJ ŚRODOWISKA SKALNEGO

Słowa kluczowe

Zbiorniki węglowodorów, powierzchniowe pomiary sejsmiczne, rozkład pseudoimpedancji akustycznej, analiza danych i ich wizualizacja, kontekstowe i adaptacyjne transformacje obrazów, interpretacja struktury przekrojów skalnych, wykrywanie niejednorodności pokładów soli.

Streszczenie

Podziemne zbiorniki węglowodorów pełnią ważną rolę we współczesnym świecie. Większość z nich jest lokalizowana w opróżnionych zbiornikach gazu ziemnego. Złoża soli kamiennej o jednorodnej wewnętrznej strukturze i poziomym lub prawie poziomym warstwowaniu stwarzają doskonałe warunki dla lokalizacji planowanych podziemnych zbiorników węglowodorów. W pokładach soli, jednorodność, zmiany litologii i miąższości pokładu, powinny być dokładnie rozpoznane przed podjęciem decyzji o lokalizacji zbiornika. Powierzchniowe pomiary sejsmiczne są ekonomicznym źródłem niezbędnych informacji. Wykonanie inwersji sekcji sejsmicznych prowadzi do uzyskania przybliżonego rozkładu impedancji akustycznej. Dane takich rozkładów są bazą do tworzenia obrazów i wizualnej interpretacji budowy ośrodka skalnego. Detekcja niejednorodności litologiczno-facjalnych w budowie pokładowych złóż soli może być rozpoznawana na podstawie właściwej interpretacji obrazów sekcji pseudoimpedancji akustycznej. W artykule wykorzystano metodę dekonwolucji minimum entropii dla polepszenia rozdzielczości obrazów sekcji geologicznych. Zaproponowano również przekształcenia kontekstowe i adaptacyjne obrazów dla zwiększenia efektywności poprawnej interpretacji obrazów symulowanych przez system INWERS. Przedstawiono algorytm przekształceń wizualizacji i analizy wyników określającej jakość interpretacji budowy ośrodka skalnego Praca ma na celu rozwój zastosowań narzędzi obróbki obrazów do wykrywania niejednorodności zmian litologiczno-facjalnych struktury w poziomych pokładach soli kamiennej.